Coarse, fast, and still accurate? Comparing corrections for the actuator line model

Korb, Henry; Taschner, Emanuel

DOI
10.1088/1742-6596/3016/1/012051

Publication date
2025

Document Version
Final published version

Published in
Journal of Physics: Conference Series

Journal of Physics:
Conference Series

PAPER • **OPEN ACCESS**

Coarse, fast, and still accurate? Comparing corrections for the actuator line model

To cite this article: Henry Korb and Emanuel Taschner 2025 *J. Phys.: Conf. Ser.* **3016** 012051

Journal of Physics: Conference Series **3016** (2025) 012051 doi:10.1088/1742-6596/3016/1/012051

Coarse, fast, and still accurate? Comparing corrections for the actuator line model

Henry Korb[1] **and Emanuel Taschner**[2]

[1] Department of Earth Sciences, Uppsala University, Visby, Sweden
[2] Delft Center for Systems and Control, Delft University of Technology, Delft, The Netherlands

E-mail: henry.korb@geo.uu.se

Abstract. The actuator line method for modeling wind turbine blades in wind farm flow simulations often offers a good compromise between accuracy and computational cost. A variety of methods have been proposed to correct the force prediction by the actuator line near the tip and root due to smearing the force in the flow domain. This article compares the two most commonly used methods (the filtered lifting line and the vortex-based smearing correction) in terms of accuracy, applicability and computational performance. Both corrections perform well for a single turbine, significantly reducing the force and power overprediction. The effect on power is larger than on thrust. Applying the corrections leads to more accurate results even at lower resolutions. The application of the corrections in an ALM simulation of a wind farm with 30 turbines reduces power by up to 10% compared to a case without correction. Different turbines in the farm are affected differently. The improvements in accuracy due to the corrections far outweigh the additional computational cost.

1 Introduction

The actuator line method (ALM), introduced by Sørensen and Shen [1], is an efficient model to compute the interaction of wind turbines and the surrounding flow in large eddy simulation (LES) when individual blades should be captured, but body-resolving grids are computationally prohibitive. However, it is well known that the ALM leads to an overprediction of the forces acting on the turbine, and thus an overestimation of power production and thrust, which increases with coarser resolution [2]. In light of the growing size of wind farms, computational cost of wind farm simulations increases drastically, often allowing only coarse resolutions. Nevertheless the model fidelity of the ALM might still be required, e.g. in order to study control strategies leveraging individual pitch control such as the helix [3]. For these application cases both accurate power prediction as well as estimation of turbine fatigue loads remain crucial for the optimization of the controller. Hence, corrections to reduce the resolution requirement of the ALM without exacerbating the power overprediction are well sought-after and a steady stream of improvements to the ALM have been proposed, with varying degrees of physical and empirical reasoning [4, 5].

In the original formulation of the ALM, lift and drag forces acting on the blades are computed from tabulated airfoil data and are imposed on the flow as body forces. In order to improve numerical stability, the forces are smeared in the flow domain via convolution with a regularization kernel. Extensive investigations of the classical formulation, which uses an isotropic Gaussian kernel with width ϵ, were carried out in Troldborg [6] and Martínez-Tossas et al. [2]. Troldborg [6] recommends a smearing width of twice the cell width to minimize the effect of smearing while avoiding numerical instabilities. Examining the error in the angle of attack in Meyer Forsting and Troldborg [7] even leads to the recommendation to

use the largest smearing width possible. Martínez-Tossas et al. [8] and Meyer Forsting et al. [9] showed that the shed vorticity has the shape of the regularization kernel, which was first observed in Dağ [10]. As a consequence the induced velocity corresponding to the vorticity matches the distribution as it is found for a Lamb-Oseen vortex, where its core width is equal to the kernel width ϵ. The regularization applied in LES thus leads to an underestimation of induced velocity, since the kernel widths employed in practice exceed the physical reasonable values by at least an order of magnitude. This mismatch is the main source of the force overprediction of the ALM.

Following this observation, several correction methods have been proposed: Martínez-Tossas and Meneveau [11], Meyer Forsting et al. [9], Dağ and Sørensen [12], and Kleine et al. [13]. As shown in Kleine et al. [13], all corrections follow the same idea: the velocity induced by the regularized forces is compared to a reference induced velocity and the sampled velocities from the LES domain are corrected by the difference. Meyer Forsting et al. [9], Dağ and Sørensen [12], and Kleine et al. [13] consider an ideal lifting line solution as reference ($\epsilon_{Opt}/c = 0$), whereas Martínez-Tossas and Meneveau [11] compare to a filtered lifting line with the optimal kernel width determined in Martínez-Tossas et al. [8] as fraction of the local chord length c to be $\epsilon_{Opt}/c = \mathcal{O}(10^{-1})$. Furthermore, the approaches for computing the induced velocity and for solving the resulting equations differ. Meyer Forsting et al. [14] presents multiple options to reduce the computational cost of the correction proposed in Meyer Forsting et al. [9] and the effect of the correction on the wake was assessed in Meyer Forsting et al. [15]. The correction proposed by Martínez-Tossas and Meneveau [11] was applied in the simulation of a single turbine in Stanly et al. [16] and a generalization was presented in Martínez-Tossas et al. [17].
This work compares the corrections put forth in Meyer Forsting et al. [9] and Martínez-Tossas and Meneveau [11]. They were chosen out of the four since they are already in use in many LES codes tailored for wind energy purposes and are (relatively) simple to implement. We compare the corrections in terms of achieved accuracy, their effect on the wake of a single turbine and their added computational cost. Furthermore, we explore their range of applicability since we are ultimately interested in the feasibility of coarse, but still sufficiently accurate, ALM simulations of very large wind farms. To this end, we conduct a range of single turbine ALM-LES simulations in uniform and turbulent inflow, varying grid resolution, inflow parameters and kernel width. We then showcase the performance of the corrections for a wind farm of thirty turbines operating in a neutral pressure-driven boundary layer (PBL). The paper is structured as follows: in section 2 we introduce the corrections as well as the employed LES solver and set-up; we present and discuss the results in section 3; and conclude in section 4.

2 ALM Corrections and Numerical Simulation Methodology

In the following section we briefly introduce the two different ALM correction models, which are compared in this study as well as the general methodology of the performed large-eddy simulations. We start by defining the problem setup in Figure 1.

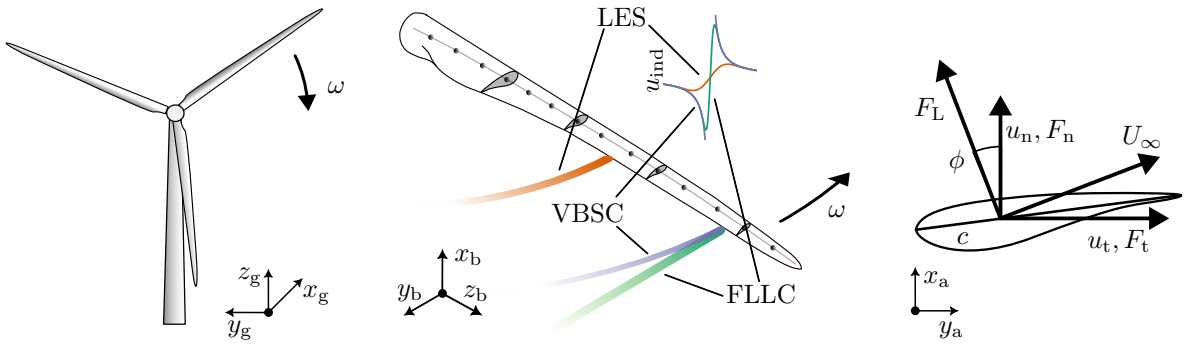

Figure 1: Problem setup showing the definitions of the global $\mathcal{K}_g(x_g, y_g, z_g)$, the blade-attached $\mathcal{K}_b(x_b, y_b, z_b)$ and the local airfoil $\mathcal{K}_a(x_a, y_a, z_a)$ coordinate system. Normal and tangential forces (F_n and F_t) and the lift and drag forces (F_L and F_d) are related via the local flow angle ϕ. Vorticity shed and velocity induced by ALM are shown in orange; the respective optimal reference vortex and reference induced velocity taken by the FLLC and VBSC corrections are shown in green and purple.

2.1 Corrections for the actuator line model

2.1.1 Filtered lifting line correction (FLLC) The underlying idea of the FLLC is the computation of two different induced velocity solutions along the blade span — one corresponding to the Gaussian kernel width ϵ_{LES} employed in the LES, the other corresponding to the optimal reference ϵ_{Opt} [11]. These two solutions are obtained by numerically solving a convolution integral for the induced velocity [17]. This integral solution is derived from the linearised inviscid vorticity transport equation subject to the ALM point forces regularized with a Gaussian kernel. The only required input to this solution is the instantaneous spanwise lift distribution $\boldsymbol{F}_{\mathrm{L}} = (F_{\mathrm{L},x_{\mathrm{b}}}, F_{\mathrm{L},y_{\mathrm{b}}}, 0)^T$ sampled at the actuator points (expressed in $\mathcal{K}_{\mathrm{b}}$). The corresponding induced velocity $\boldsymbol{u}_{\mathrm{ind}}(t;\epsilon_i)$ at each actuator point (and also expressed in the blade-attached coordinate system) is then obtained by solving the aforementioned integral

$$\boldsymbol{u}_{\mathrm{ind}}(t;\epsilon_i) = -\frac{1}{2\pi}\int_{R_{\mathrm{r}}}^{R_{\mathrm{t}}} \frac{\boldsymbol{F}_{\mathrm{L}}(z'_{\mathrm{b}})}{|U_\infty(z'_{\mathrm{b}})|\,\epsilon_i(z'_{\mathrm{b}})^2}\left[e^{\frac{-(z'_{\mathrm{b}}-z_{\mathrm{b}})^2}{\epsilon_i(z'_{\mathrm{b}})^2}} + \frac{\epsilon_i(z'_{\mathrm{b}})^2}{2(z'_{\mathrm{b}}-z_{\mathrm{b}})^2}\left(e^{\frac{-(z'_{\mathrm{b}}-z_{\mathrm{b}})^2}{\epsilon_i(z'_{\mathrm{b}})^2}} - 1\right)\right]\mathrm{d}z'_{\mathrm{b}} \qquad (1)$$

for $\epsilon_i \in \{\epsilon_{\mathrm{LES}}, \epsilon_{\mathrm{Opt}}\}$, where R_{r} and R_{t} denote the blade root and tip location. In the LES the blade is represented by N_{Act} discrete actuator points. For the computationally efficient evaluation of the above integral it is beneficial to use a non-uniform distribution of actuator points with a denser spacing in regions of large lift gradients, i.e. at the tip and root. The discrete points z_{b}^k are placed such that the point spacing is constant with respect to the locally optimal kernel width $\Delta z_{\mathrm{b}}^k/\epsilon_{\mathrm{Opt}}^k = const.$ In principle equation 1 represents an integral equation where $\boldsymbol{F}_{\mathrm{L}} = \boldsymbol{F}_{\mathrm{L}}(\boldsymbol{u}_{\mathrm{ind}})$. While it can be solved standalone by reformulating it as a root finding problem [18], the implementation in an LES code with explicit time stepping requires a successive convergence across multiple time steps, which is achieved using under relaxation of the correction term $\boldsymbol{u}_{\mathrm{ind}}(\epsilon_{\mathrm{Opt}}) - \boldsymbol{u}_{\mathrm{ind}}(\epsilon_{\mathrm{LES}})$ (the relaxation factor in this study is $f_{\mathrm{u}} = 0.1$).

2.1.2 Vortex-based smearing correction (VBSC) The vortex-based smearing correction as presented in Meyer Forsting et al. [9] also computes two induced velocities to correct the velocity sampled from the LES. However, both velocities differ from the FLLC. The velocity induced from the vortices shed by the actuator line is computed from the near-wake model for trailed vorticity presented in Pirrung et al. [19]. The near-wake model has to be solved iteratively for each blade. The VBSC then computes the difference in induction to the induction of an inviscid vortex and corrects the sampled velocities. The VBSC performs well even with few actuator points and a variety of methods for improving its performance were presented in [14]. While the implementation of the VBSC is significantly more cumbersome than that of the FLLC, it imposes fewer restrictions on the user in terms of actuator points. It should also be noted that the FLLC since it does not require any iterative solution at each time step can be used for ALM implementations coupled to multi-physics turbine modeling codes like OpenFAST [20]. Such a coupling is not straightforward using the VBSC.

2.2 LES model and simulation cases

This study uses the GPU-resident Lattice Boltzmann solver `VirtualFluids`[1] to simulate the flow field. We employ the highly stable and accurate cumulant LBM as described in Geier et al. [21]. The ALM forces are calculated with `wiFI` [2]. The methodology is described in more detail and validated in [22].

2.2.1 Single turbine parameter study We study the effect of grid resolution and kernel width, examining the turbine response and wake of a single NREL 5MW reference turbine [23] with diameter $D = 126\,\mathrm{m}$. The flow domain has a size of $24D \times 8D \times 8D$ in x_{g}, y_{g}, and z_{g} direction, respectively. The turbine is placed three diameters downstream of the inflow boundary and is centered in y_{g} and z_{g}. Lateral boundaries are periodic, the inflow boundary is a bounce-back condition equivalent to a velocity boundary condition and the outflow boundary is a non-reflective outflow boundary. We vary the grid resolution and kernel width between $\Delta x = D/16, D/24, D/32$ and $\epsilon = D/8, D/12, D/16$, respectively. We conduct simulations of all possible combinations of these parameters with uniform inflow. These values represent ALM coarse grid scenarios for which we compare the ability of the corrections to improve accuracy. The parameters of all simulations are gathered in Table 1. The commonly used measure $\epsilon/\Delta x$ as it results from the studied grid resolutions and kernel widths is shown in Table 2. Furthermore, we conduct simulations with 5% and 10% inflow turbulence from synthetically generated turbulence [24] for the combination of the finest resolution and smallest kernel width. In addition, we conduct a single simulation at a high grid resolution

[1] `https://git.rz.tu-bs.de/irmb/VirtualFluids`

[2] `https://source.coderefinery.org/hkorb/wifi`

Table 1: Overview of the conducted single turbine reference case, the parametric single turbine study and the wind farm test case. The details shown are LES grid resolution, kernel width employed in the LES, physical optimality ϵ_{LES}/c_{Tip}, number of actuator points along the blade (depends on the type of correction), inflow type and the type of applied corrections (from left to right).

$D/\Delta x$	$D/\epsilon_{\mathrm{LES}}$	$\epsilon_{\mathrm{LES}}/c_{\mathrm{Tip}}$	N_{Act}	Inflow	Correction
196	49	2.9	400	uniform	None
16	16	9	32/79/32	uniform	None/FLLC/VBSC
16	12	12	32/79/32	uniform	None/FLLC/VBSC
16	8	18	32/79/32	uniform	None/FLLC/VBSC
24	16	9	32/79/32	uniform	None/FLLC/VBSC
24	12	12	32/79/32	uniform	None/FLLC/VBSC
24	8	18	32/79/32	uniform	None/FLLC/VBSC
32	16	9	32/79/32	uniform	None/FLLC/VBSC
32	12	12	32/79/32	uniform	None/FLLC/VBSC
32	8	18	32/79/32	uniform	None/FLLC/VBSC
32	16	9	32/79/32	synthetic ($TI = 5\%$)	None/FLLC/VBSC
32	16	9	32/79/32	synthetic ($TI = 10\%$)	None/FLLC/VBSC
24	12	12	32	PBL ($TI_{\mathrm{hub}} = 5\%$)	None/FLLC/VBSC

Table 2: Interdependence of the ratio $\epsilon_{\mathrm{LES}}/\Delta x$ on the numerical convergence of the force regularization (refining Δx for constant ϵ) and the degree of physical optimality (increases for smaller ϵ_{LES}/c_{Tip}) for the nine cases of the parameter study. Moving towards the bottom right in the shown parameter space increases both numerical and physical convergence.

physical optimality, $\Delta x = const$ $\longrightarrow$

numerical convergence $\epsilon_{LES} = const$ $\longleftarrow$ $D/\Delta x$	D/ϵ = 8	12	16
16	2	4/3	1
24	3	2	3/2
32	4	8/3	2

to serve as reference case, the parameters of this case can be found in the first row of Table 1. We employ three layers of refinement to reach a resolution of $\Delta x = D/196 \approx 0.64\,\mathrm{m}$ and discretize the actuator line with 400 nodes. Turbines operate at a constant rotational speed ω depending on the tip-speed ratio $\lambda = \frac{\omega R}{U_0} = 7.55$, where R is the tip-radius of the blade and $U_0 = 8\,\mathrm{m/s}$ is the inflow velocity. Lastly, we also compute the force profiles and thrust/power coefficients predicted by blade element momentum theory (BEM) for the given operating point. Simulations are conducted for 1000 s, comprising a spin-up time of 400 s and a measurement time of 600 s. Measurements are taken with a frequency of 1 Hz.

2.2.2 Wind farm in neutral pressure-driven boundary layer (PBL) As we aim to judge the correction comparisons from the perspective of applicability, we have to test them in a realistic scenario, i.e. the simulation of a wind farm. We simulate a farm comprising 6 rows of 5 NREL 5MW turbines in an aligned setup. Turbines are controlled with the standard controller described in Jonkman et al. [23]. We simulate the flow according to the precursor-successor methodology validated in Korb et al. [22]. The precursor has a spin-up time of 24 h and the successor simulation is run for 2 h. Both precursor and successor have a width of $40D$ and height of $10D$. The successor has a length of $60D$ to accommodate the wind farm while the precursor only requires a length of $40D$. The domain has a resolution of $\Delta x = D/12$ and the grid is refined by a factor of two around the farm. We employ a wall model at the bottom boundary with roughness length $z_0 = 1 \times 10^{-3}\,\mathrm{m}$. The flow is driven with a constant pressure gradient such that the wall shear stress corresponds to a friction velocity $u_* = 0.29\,\mathrm{m/s}$, resulting in a hub height velocity $u_h \approx 8.4\,\mathrm{m/s}$. The inflow has a turbulence intensity at hub height of $TI_{\mathrm{hub}} = 5.7\%$. We conduct successor simulations without correction and both corrections, where averages are computed using the last 1 h of data sampled with a frequency of 1 Hz, which is sufficiently long to obtain converged statistics.

3 Accuracy improvement and computational cost of the ALM corrections

3.1 Uniform inflow

In order to examine the connection of kernel width and grid resolution, we first focus on the set of nine simulations with uniform inflow. Spanwise force profiles for the resolution of $\Delta x = D/32$ and the three different kernel widths are shown in Figure 2. First, we note that the forces from the reference simulation and the BEM model agree closely for $r/R < 0.8$ but are not an exact match close to the blade tip. This can be partially due to differing assumptions of the two models [25], but also due to the fact that for our reference simulations $\epsilon_{\mathrm{LES}}/c_{\mathrm{Tip}}$ in the tip region is still an order larger than the optimal ratio. This further highlights the prohibitive cost of the ALM with optimal kernel widths and the need for effective corrections. We can clearly observe that the normal and tangential forces F_{n} and F_{t} match the expected results from the reference solution closely in the middle section of the blade in all cases. However, if no correction is used, the well-known overprediction of forces in the tip region is observed, where the overprediction decreases with smaller kernel width. If we apply either correction we find good agreement with the reference for all three grid resolutions for $r/R < 0.8$. At the tip the FLLC perfectly matches the BEM solution except for the spike at the tip. This spike predicted by the FLLC is a physical results of taking a very small but non-zero kernel width as reference for the correction of the induced velocity. In contrast, the VBSC assumes an ideal point vortex solution as reference. The associated velocity singularity of this reference drives the forces smoothly towards zero as $r/R \to 1$. The VBSC predicts smaller forces than BEM close to the tip.

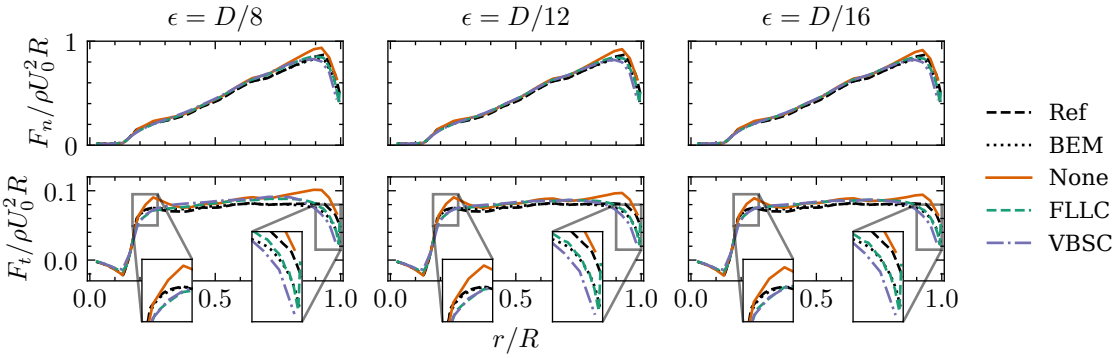

Figure 2: Mean line forces along the blade for simulations with $D/\Delta x = 32$ and varying kernel width.

Figure 3 shows the wake deficits at various downstream locations for the same cases as Figure 2. The plot shows that the smearing width has a large influence on the shape of the wake deficit, while the correction methods have little influence, which also had been observed in Meyer Forsting et al. [15]. It should be pointed out that even with corrections the ALM forces are still projected onto the LES grid with the suboptimal large kernel width. Thus the effect of the corrections on the wake is expected to be weaker compared to their impact on turbine forces. We find acceptable results for both $\epsilon = D/16$ and $\epsilon = D/12$, however at $\epsilon = D/8$ the wake shape is significantly different and wake recovery is significantly slower. The larger kernel widths create a weaker wake shear layer which in turn delays laminar-turbulent transition in the wake ultimately delaying wake recovery [2].

To condense all the previously discussed results as well as the effect of employing the different corrections on runtime, we show heatmaps of error in power, thrust, and rotor equivalent wind speed U^{eq} at $x = 10D$, as well as the realtime factor in Figure 4. Error in power and thrust are given relative to the values computed from BEM, while the rotor equivalent wind speed is compared to the results from the reference simulation. The uncorrected ALM predicts up to 20% more power than the BEM reference, and even at the highest resolution yields more than 13% more power. The error decreases with higher resolution and smaller smearing width. When using a correction, the error can be reduced significantly, even at low resolutions. The VBSC error is consistently lower than that of the FLLC although differences are not large. Referring to the force profiles in Figure 2 the VBSC overpredicts/underpredicts BEM results blade inwards/outwards, which can lead to integral smaller error due to error cancellation. The same observations can be made for the thrust. Interestingly, the case with the lowest error is not the case with $\epsilon = D/16$ but $\epsilon = D/12$, possibly due to lower error in the computation of the angle of attack as was discussed in [7]. It should be noted here that comparison between different kernel widths at a fixed resolution is also impacted by varying ratios of $\epsilon/\Delta x$ (see Table 2). The third column shows again

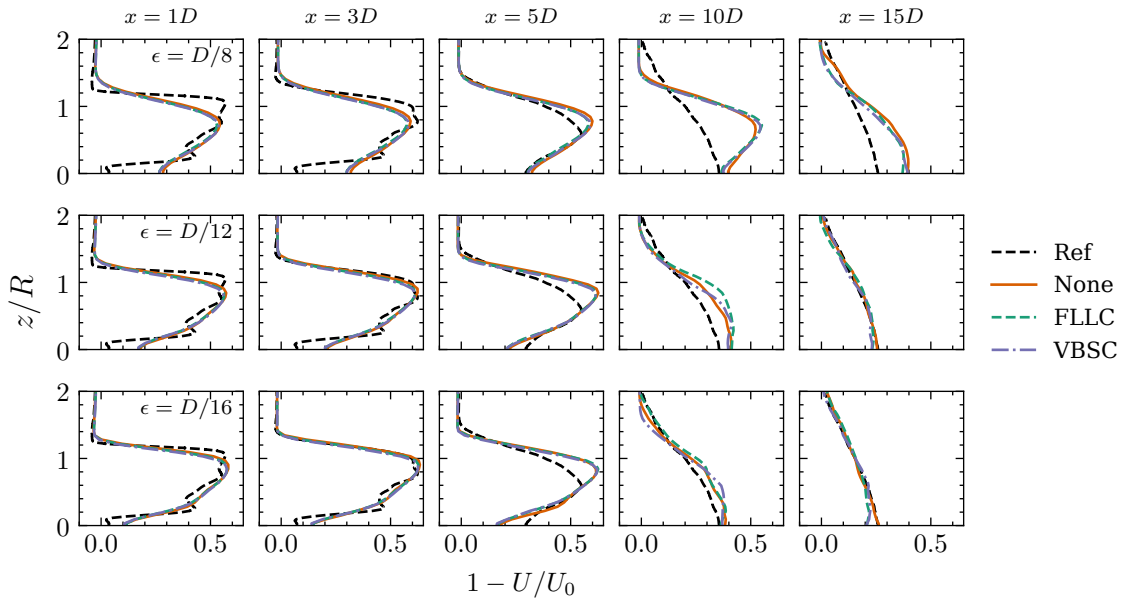

Figure 3: Wake deficit profiles of simulations with $D/\Delta x = 32$.

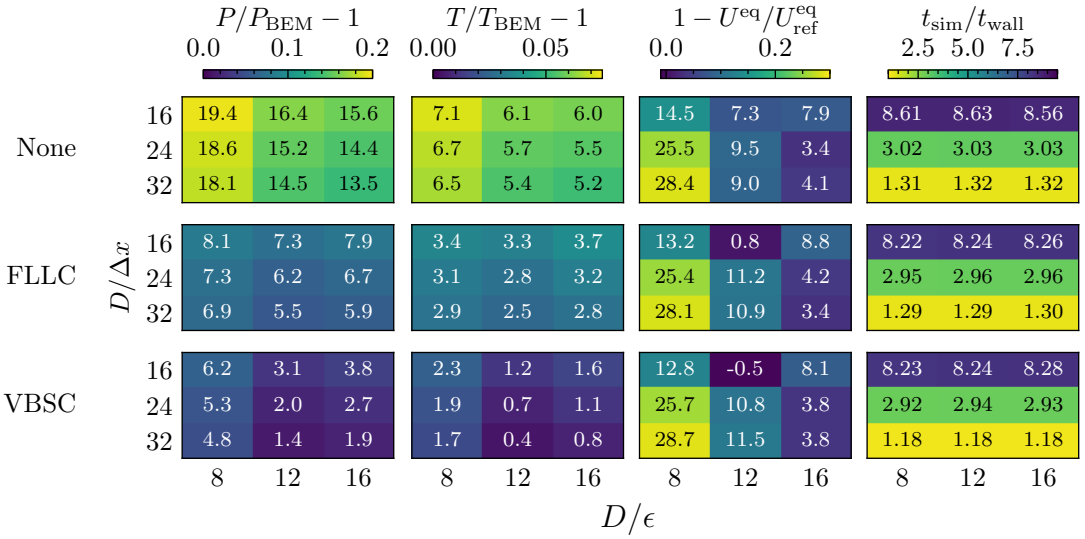

Figure 4: Heatmap of results from the parameter study. From left to right: error in turbine power; error in thrust; error in rotor equivalent wind speed at $x = 10D$, realtime factor as simulated time t_{sim} over wall time t_{wall}. Numbers in the first three columns of plots are given in percent. The rotor equivalent wind speed is computed as $U^{eq} = \left(\frac{1}{N}\sum_i u_i^3\right)^{1/3}$ [26].

that the effect of employing a correction on the wake are significantly lower, however reducing the kernel width has a far larger effect. Increasing resolution from $\Delta x = D/16$ to $\Delta x = D/24$ reduces the error significantly, while further increase in resolution does not. This is generally in line with Martínez-Tossas et al. [2]. There is no discernable difference between FLLC and VBSC. We choose to display U^{eq} at $x = 10D$ to emphasize the effect on transition, which occurs significantly later in uniform inflow than in turbulent inflow. The very low error for the cases with $D/\Delta x = 16$ and $D/\epsilon = 12$ is due to a favourable cancellation of errors. Finally, we see that both corrections have some computational overhead, usually below 5% of the overall wall time, only at high resolutions the overhead of the VBSC does reach up

to 10%. However, the impact of increasing resolution on the computational cost is significantly larger. We want to emphasize that the wall time measurements are obviously specific to implementation and hardware used. Figure 4 shows, that even at ten times higher computational cost, the uncorrected ALM has a much larger error in power and thrust prediction than obtain from either correction.

3.2 Turbulent inflow

To examine the robustness of the correction methods under varying inflow conditions, we conduct simulations with synthetic turbulent inflow of 5% and 10% turbulence intensity. The resulting line forces are shown in Figure 5, with averages shown as lines and two standard deviations shaded. Both corrections still perform well and the same trends as in uniform flow are observed, albeit that the computed tangential force agrees closer with BEM results across all cases. Furthermore, we observe larger differences of forces between ALM and BEM inboard of the blade with higher turbulence intensity. Again, we find little difference between the two corrections with the exception of a spike in tangential force computed by the FLLC.

Figure 6 shows how the corrections change the normal and tangential velocities, u_n and u_t, respectively. Both corrections mainly act at the root and tip and we can clearly observe the shape of the induced velocity by a vortex. The FLLC predicts smaller peak velocities, since the underlying assumption is that an optimal actuator line sheds a vortex with finite core width $\epsilon/c = \mathcal{O}(10^{-1})$ for which the induced velocity at the vortex center is zero, whereas the VBSC assumes a singular point vortex with infinitesimally small core size for which the induced velocity possess a singularity at the vortex center.

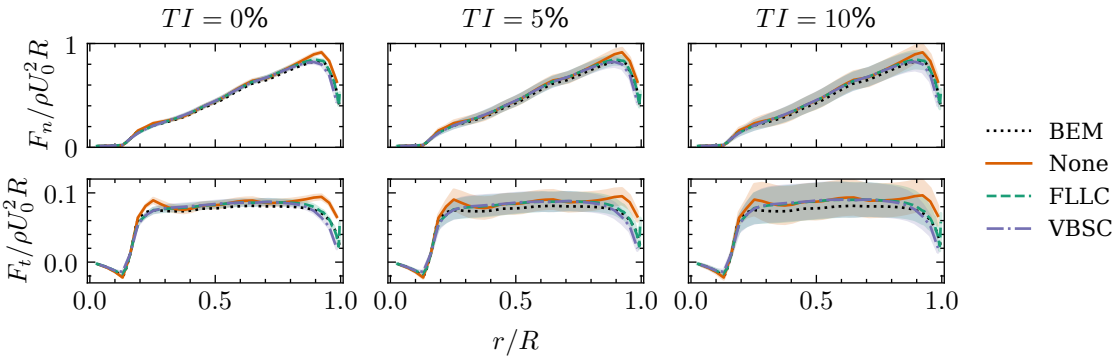

Figure 5: Mean line forces along the blade for simulations with $D/\Delta x = 32$ for varying turbulence intensity. The shaded area shows ± 1 standard deviation.

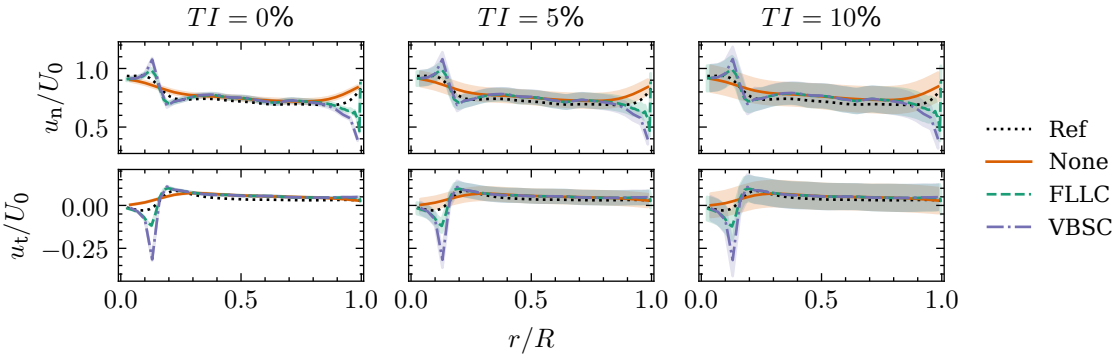

Figure 6: Mean corrected velocities sampled by the ALM for simulations with $D/\Delta x = 32$ for varying turbulence intensity. The shaded area shows ± 1 standard deviation.

C_P and C_T for the three different inflow turbulence levels are shown in Figure 7. We find consistently higher values for both coefficients compared to the BEM reference. Both corrections improve the results,

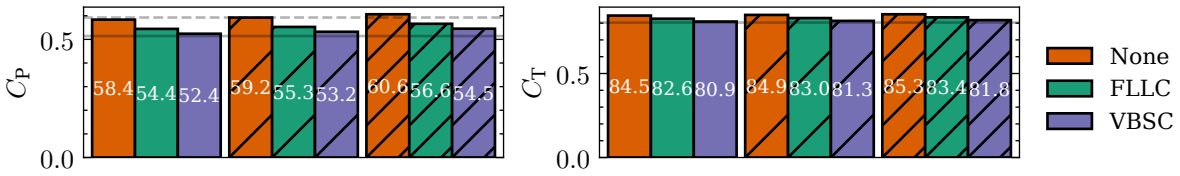

Figure 7: C_P and C_T of simulations with uniform (not hatched) and turbulent inflow (hatched 5%, double hatched 10%). Results from BEM in solid grey. Betz limit of C_P in dashed grey.

with the VBSC being the closest to the reference. The differences become more pronounced with higher turbulence intensity. At high turbulence intensities the turbine even exceeds the Betz limit, if no correction is used. Figure 7 demonstrates that an accurate power prediction requires the use of an ALM correction, otherwise the power coefficient can be overestimated by 10%.

3.3 Wind farm in a neutral pressure-driven boundary layer

Lastly, we aim to evaluate the performance of the smearing corrections in a realistic use case of a wind farm in a neutral pressure-driven boundary layer. Since previous results showed little effect of the corrections on the flow, we omit the results here for brevity´s sake and instead only show the average power and thrust coefficient in the wind farm as well as realtime factor in Figure 8. As indicated by previous results, both corrections mostly affect the power coefficient. Both corrections yield similar results, but the VBSC yields a slightly larger reduction. The $\overline{C}_P$ of the VBSC is 88% of the uncorrected, while application of the FLLC results in a $\overline{C}_P$ of 91%. The thrust coefficient is reduced by 3% and 5% by FLLC and VBSC, respectively. Lastly, we show the computational cost associated with applying a correction model. The FLLC results in an increase of 2% in computational time, while the VBSC increases computational time by 4%.

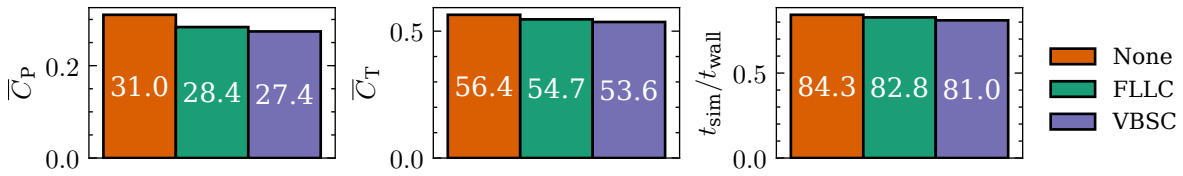

Figure 8: Average power and thrust coefficient as well as simulated time to wall time for the wind farm in NPBL.

A more detailed view of the effect of the corrections is given in Figure 9, showing the power and thrust of the simulations with both corrections relative to the simulation without correction. The VBSC has

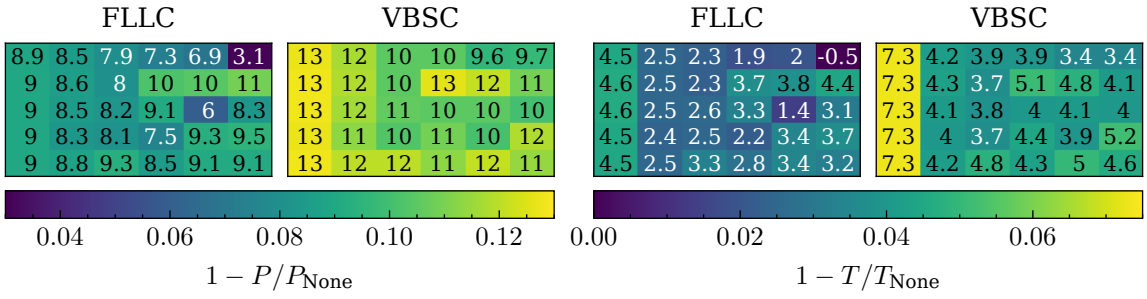

Figure 9: Change in power and thrust per turbine compared to the wind farm simulation without correction. The first row of turbines in the farm (most upstream) corresponds to the column furthest left in the plot. Numbers given in percent.

the strongest effect in the first row, reducing power by 13% and thrust by 7.3 %, however some turbines downstream are also strongly affected, with no particular pattern. The FLLC has an even more irregular pattern. The strongest reduction in power is found in the last row, while the least affected turbine is right next to it. Generally, power is more affected than thrust and the VBSC yields higher reductions than the FLLC. Figure 9 shows that the power prediction of the ALM cannot simply be corrected by a constant factor determined from a standalone simulation, further highlighting the importance of the correction methods.

4 Conclusion

We compared two correction methods for the actuator line method, the filtered lifting line correction and the vortex-based smearing correction, in terms of performance, applicability and computational cost. We conducted a parameter study in uniform inflow, varying kernel width and grid resolution, used synthetically generated turbulent inflow and simulated a wind farm in a neutral pressure-driven boundary layer. We find that the two tested corrections reliably reduce the effect of the force regularization under all conditions but perform best at higher resolutions. The average power coefficient of the wind farm was reduced by up to the order 10% when applying a correction model, while the computational overhead was limited to 4%.

The parameter study in uniform inflow examines nine cases of a single turbine with three different resolutions and three kernel widths. Each case is simulated with both corrections and a reference simulation without correction. For reference we also simulate a very highly resolved actuator line. We find that both corrections reduce the overprediction of forces at the tip and root of the blade. Without correction, the power coefficient of a single turbine is 10% to 20% higher than the coefficient computed with BEM. Both corrections reduce the difference to below 10% in all cases. The vortex based smearing correction is consistently closer to the reference, however the differences are small. The effect on the rotor equivalent wind speed ten diameters downstream of the turbine is smaller, kernel width and resolution have a significantly higher influence. Curiously, the best results are obtained at low resolution and small kernel width. However, this is due to the sensitivity of the location of transition from near to far wake to the simulation setup and can change in turbulent flow conditions. The runtime increases between 2% and 10%, depending on case and correction. At high resolutions, the vortex-based smearing correction is more expensive than the filtered lifting line.

Both corrections consistently provide good results also in turbulent inflow at 5% and 10% turbulence intensity, yielding lower power and thrust coefficients than the uncorrected simulation. Examination of the corrected velocities shows that both corrections mainly correct for the missing induction due to weakened root and tip vortex.

Finally, we examined the average power and thrust coefficient of a wind farm comprising 30 wind turbines. We find that the average power coefficient is reduced by 9% and 12% by the filtered lifting line and vortex-based smearing correction, respectively, while the computational time only increases by 2% and 4%, respectively. The thrust coefficient is only reduced by 3% and 5%. However, the reduction in power and thrust is not consistent across all turbines, nor do both corrections affect the same turbines with the same strength. It is therefore not sufficient to simply correct the power prediction of an actuator line by a constant factor.

In summary, we find both corrections improve the accuracy of the actuator line method. Overall, the great improvement of accuracy of both methods compensates the small computational overhead imposed by employing either correction. Thus, the use of such corrections can significantly reduce the computational cost by reducing the flow resolution while actually improving accuracy, especially in power prediction. Each method has advantages and disadvantages: The filtered lifting line is simpler to implement and computationally more efficient, however, it requires a higher number of actuator points even when using a non-uniform point distribution. The vortex-based smearing corrections seems more accurate, however the differences are not large and can be influenced by fortunate error cancellation when considering integral quantities like thrust and power. In light of the great practical application, these smearing corrections could be improved with further research. For example, it is not clear, what exactly the influence of the underlying assumptions is. In principal, both methods could also work with "the other" reference induction.

Acknowledgements:
E.T.'s PhD project is part of the Hollandse Kust Noord wind farm innovation program where CrossWind C.V., Shell, Eneco, Siemens Gamesa and GROW are teaming up; funding for the PhDs and PostDocs was provided by CrossWind C.V. and Siemens Gamesa.

References

[1] JN Sørensen and WZ Shen. "Numerical Modeling of Wind Turbine Wakes". In: *Journal of Fluids Engineering* 124.2 (2002), pp. 393–399. DOI: 10.1115/1.1471361.
[2] LA Martínez-Tossas, MJ Churchfield, and S Leonardi. "Large Eddy Simulations of the Flow Past Wind Turbines: Actuator Line and Disk Modeling". In: *Wind Energy* 18.6 (2015), pp. 1047–1060. DOI: 10.1002/we.1747.
[3] JA Frederik et al. "The Helix Approach: Using Dynamic Individual Pitch Control to Enhance Wake Mixing in Wind Farms". In: *Wind Energy* 23.8 (2020), pp. 1739–1751. DOI: 10.1002/we.2513.
[4] WZ Shen et al. "Tip Loss Corrections for Wind Turbine Computations". In: *Wind Energy* 8.4 (2005), pp. 457–475. DOI: 10.1002/we.153.
[5] JN Sørensen, KO Dağ, and N Ramos-García. "A Refined Tip Correction Based on Decambering". In: *Wind Energy* 19.5 (2016), pp. 787–802. DOI: 10.1002/we.1865.
[6] N Troldborg. "Actuator Line Modeling of Wind Turbine Wakes". PhD thesis. 2009.
[7] AR Meyer Forsting and N Troldborg. "Generalised Grid Requirements Minimizing the Actuator Line Angle-of-Attack Error". In: *Journal of Physics: Conference Series* 1618.5 (2020), p. 052001. DOI: 10.1088/1742-6596/1618/5/052001.
[8] LA Martínez-Tossas, MJ Churchfield, and C Meneveau. "Optimal Smoothing Length Scale for Actuator Line Models of Wind Turbine Blades Based on Gaussian Body Force Distribution". In: *Wind Energy* 20.6 (2017), pp. 1083–1096. DOI: 10.1002/we.2081.
[9] AR Meyer Forsting, GR Pirrung, and N Ramos-García. "A Vortex-Based Tip/Smearing Correction for the Actuator Line". In: *Wind Energy Science* 4.2 (2019), pp. 369–383. DOI: 10.5194/wes-4-369-2019.
[10] KO Dağ. "Combined Pseudo-Spectral / Actuator Line Model for Wind Turbine Applications". PhD thesis. 2017.
[11] LA Martínez-Tossas and C Meneveau. "Filtered Lifting Line Theory and Application to the Actuator Line Model". In: *Journal of Fluid Mechanics* 863 (2019), pp. 269–292. DOI: 10.1017/jfm.2018.994.
[12] KO Dağ and JN Sørensen. "A New Tip Correction for Actuator Line Computations". In: *Wind Energy* 23.2 (2020), pp. 148–160. DOI: 10.1002/we.2419.
[13] VG Kleine, A Hanifi, and DS Henningson. "Non-Iterative Vortex-Based Smearing Correction for the Actuator Line Method". In: *Journal of Fluid Mechanics* 961 (2023), A29. DOI: 10.1017/jfm.2023.237.
[14] AR Meyer Forsting, GR Pirrung, and N Ramos-García. "Brief Communication: A Fast Vortex-Based Smearing Correction for the Actuator Line". In: *Wind Energy Science* 5.1 (2020), pp. 349–353. DOI: 10.5194/wes-5-349-2020.
[15] AR Meyer Forsting, GR Pirrung, and N Ramos-García. "The Wake of an Actuator Line with a Vortex-Based Tip/Smearing Correction in Uniform and Turbulent Inflow". In: *Journal of Physics: Conference Series* 1256.1 (2019), p. 012020. DOI: 10.1088/1742-6596/1256/1/012020.
[16] R Stanly et al. "Large-Eddy Simulation of a Wind Turbine Using a Filtered Actuator Line Model". In: *Journal of Wind Engineering and Industrial Aerodynamics* 222 (2022), p. 104868. DOI: 10.1016/j.jweia.2021.104868.
[17] LA Martínez-Tossas et al. "Generalized Filtered Lifting Line Theory for Arbitrary Chord Lengths and Application to Wind Turbine Blades". In: *Wind Energy* 27.1 (2024), pp. 101–106. DOI: 10.1002/we.2872.
[18] LA Martinez-Tossas et al. "A Solution Method for the Filtered Lifting Line Theory". In: *Journal of Fluids Engineering* 147.011502 (2024). DOI: 10.1115/1.4066296.
[19] GR Pirrung, HA Madsen, and S Schreck. "Trailed Vorticity Modeling for Aeroelastic Wind Turbine Simulations in Standstill". In: *Wind Energy Science* 2.2 (2017), pp. 521–532. DOI: 10.5194/wes-2-521-2017.
[20] E Taschner et al. "A New Coupling of a GPU-resident Large-Eddy Simulation Code with a Multiphysics Wind Turbine Simulation Tool". In: *Wind Energy* 27.11 (2023), pp. 1152–1172. DOI: 10.1002/we.2844.
[21] M Geier, A Pasquali, and M Schönherr. "Parametrization of the Cumulant Lattice Boltzmann Method for Fourth Order Accurate Diffusion Part I: Derivation and Validation". In: *Journal of Computational Physics* 348 (2017), pp. 862–888. DOI: 10.1016/j.jcp.2017.05.040.
[22] H Korb, H Asmuth, and S Ivanell. "Validation of a Lattice Boltzmann Solver Against Wind Turbine Response and Wake Measurements". In: *Journal of Physics: Conference Series* 2505.1 (2023), p. 012008. DOI: 10.1088/1742-6596/2505/1/012008.
[23] J Jonkman et al. *Definition of a 5-MW Reference Wind Turbine for Offshore System Development*. Tech. rep. NREL/TP-500-38060. National Renewable Energy Laboratory, 2009.
[24] J Liew, R Riva, and T Göçmen. "Efficient Mann Turbulence Generation for Offshore Wind Farms with Applications in Fatigue Load Surrogate Modelling". In: *Journal of Physics: Conference Series* 2626.1 (2023), p. 012050. DOI: 10.1088/1742-6596/2626/1/012050.
[25] L Liu et al. "Evaluating the Accuracy of the Actuator Line Model against Blade Element Momentum Theory in Uniform Inflow". In: *Wind Energy* 25.6 (2022), pp. 1046–1059. DOI: 10.1002/we.2714.
[26] R Wagner et al. "Accounting for the Speed Shear in Wind Turbine Power Performance Measurement". In: *Wind Energy* 14.8 (2011), pp. 993–1004. DOI: 10.1002/we.509.